Proximal VIS-NIR spectrometry to retrieve substance concentrations in surface waters using partial least squares modelling

A. Wagner, S. Hilgert, T. Kattenborn and S. Fuchs

ABSTRACT

Many water quality parameters such as concentrations of suspended matter, nutrients and algae directly or indirectly change the electromagnetic reflectance and transmission properties of surface water bodies. Optical measurement approaches have shown great potential to partially substitute water sampling and laboratory analyses, but are obstructed by limited flexibility or high maintenance demands. In order to overcome these problems and to bridge the gap between *in situ* and remote sensing measurements, the use of close-range, above-surface reflectance measurements in the VIS-NIR domain to measure water quality parameters in surface water bodies was investigated. Remote sensing reflectance in a 1 m^3 water tank with increasing, known concentrations of suspended solids was measured. A partial least squares model was trained to predict concentrations from reflectance curves, which performed well, considering the wide range of concentrations and illumination conditions ($R^2_{cal} = 0.96$, $R^2_{val} = 0.97$). The approach was then transferred to the field and further parameters were tested. Using a semi-autonomous spectrometer mounted to a boom stand on a motor boat, we traced substance concentrations in close intervals along a longitudinal gradient from inflow to dam in a drinking water reservoir in Brazil. The method is suitable for parameters directly influencing the reflection properties of the water body (e.g. suspended solids ($R^2_{cal} = 0.93$), chlorophyll-*a* ($R^2_{cal} = 0.74$)), or for parameters closely related to those (e.g. total phosphorus ($R^2_{cal} = 0.97$)). For chemical oxygen demand, the method is not well suited ($R^2_{cal} = 0.14$, $R^2_{val} = 0.45$). Once calibrated to the local conditions, the spectrometer can be used stationary or on moving platforms to map and monitor surface waters. The integration of the procedure into acoustic and imaging techniques is further investigated.

Key words | hyperspectral, partial least squares, proximal sensing, reservoir, suspended solids, water quality

A. Wagner (corresponding author)
S. Hilgert
S. Fuchs
Institute for Water and River Basin Management, Department of Aquatic Environmental Engineering,
Karlsruhe Institute of Technology (KIT),
Gotthardt-Franz-Str 3, 76131 Karlsruhe,
Germany
E-mail: *adrian.wagner@kit.edu*

T. Kattenborn
Institute of Geography and Geoecology,
Karlsruhe Institute of Technology (KIT),
Kaiserstr. 12, 76131 Karlsruhe,
Germany

INTRODUCTION

Due to their significance for human health and well-being, surface waters require thorough protection measures based on extensive water quality monitoring. Impacts of climate change and land use change as well as increasing usage requirements underline the need for monitoring in high spatial and temporal resolutions. Many water quality parameters such as concentrations of suspended solids, nutrients and algae directly or indirectly change the electromagnetic reflectance and transmission properties of surface water bodies. These features are increasingly used to retrieve concentrations from various substances, e.g. from recurring aerial and satellite imagery (Gholizadeh *et al.* 2016) and from stationary submerged optical sensors (Martínez-Carreras *et al.* 2016). While these methods have shown

doi: 10.2166/ws.2018.177

great potential to supplement and substitute traditional water sampling, they are obstructed by limited flexibility or high maintenance demands. Submerged, stationary optical sensors can provide continuous data for various parameters, but are subject to biofouling and subsequent drifts in recorded data as well as high sensor maintenance efforts. Remote sensing techniques have the advantage of covering spatial variations over large areas. However, ground truthing has to be accomplished within a close time-span of the satellite or airplane overpass, which limits the amount of training samples. Further limitations are the dependency on cloud-free conditions and the spatial resolution, which can be insufficient for small water bodies. In order to overcome these problems and to bridge the gap between *in situ* and remote sensing measurements, we investigate the use of close-range, above-surface reflectance measurements in the visual and near infrared (VIS-NIR) domain to measure water quality parameters in surface water bodies. Simultaneously, reference spectra for remote sensing imagery can be retrieved.

Total suspended solids (TSS) was selected as the main water quality target parameter for this study. It is, by weight and volume, the most important pollutant in the Earth's river systems (Ritchie *et al.* 2003). Also, it has proxy capabilities for nutrients, heavy metals, pesticides and pharmaceuticals, is insufficiently monitored and has great ecological and economic implications (Apitz & White 2003; Horowitz 2013). Lastly, the influence of TSS on remote sensing reflectance is well described (Ritchie *et al.* 1976; Schalles *et al.* 2001), which makes it suitable for a method development.

The goal of this study was to test a new method for the estimation of TSS concentrations from remote sensing reflectance using a relatively inexpensive and light-weight spectrometer combined with partial least squares (PLS) regression (Wold *et al.* 2001). First, results of an experimental study using a 1 m³ mesocosm and controlled TSS concentrations are outlined. Secondly, an operational application using a hyperspectral boat-mounted sensor on a Brazilian reservoir characterized by high-TSS spatial gradients is described. We additionally used the approach to estimate total phosphorus (TP), chlorophyll-*a* (chl-*a*), phycocyanin (PC), dissolved oxygen (DO) and chemical oxygen demand (COD) concentrations as well as turbidity, pH-value and Secchi disk depth (Z_{SD}). COD was chosen because the reservoir is suspected to receive untreated waste water and periodically suffers from dropping oxygen levels near the inflow. Additional parameters, relevant for drinking water reservoirs (e.g. total organic carbon, UV absorbance) could not be measured at that time.

The presented method is transferable to a variety of applications such as mobile campaign-based measurements using boats or drones, as well as stationary lake and river monitoring from buoys or bridges.

METHODS

Two setups were tested, one using a controlled mesocosm environment, the other using a boat on a reservoir. The materials and workflow are briefly described in the following.

Data acquisition of the mesocosm experiments

In order to define the potential range of TSS detection from above-water measurements, we measured remote sensing reflectance in a water tank (L × W × H: 148 × 105 × 80 cm), painted flat black. Silt and clay sediment was collected from a wet detention basin of the Weingarter Bach, the upper Rhine valley, shortly after a series of high flow events. The material was then suspended in municipal tap water using an immersion pump to create gradually increasing concentrations of TSS between 0 and 2,200 mg/L.

Hyperspectral data were acquired with an AISA+ Eagle spectrometer: a pushbroom scanner with an instantaneous field of view (IFOV) of 0.648 mRad and a field of view (FOV) of 36.04°. The AISA+ Eagle was equipped with a mirror scanner (Specim Limited, Oulu, Finland) to enable the recording of hyperspectral frames. The scanner was mounted on a scaffold at a height of 1.3 m above the water tank. We recorded scans in four times spectral binning mode to achieve an appropriate trade-off between signal-to-noise ratio and spectral resolution (Silván-Cárdenas & Wang 2010). The corresponding data features 61 spectral bands between 398 and 957 nm with a full width at half maximum (FWHM) of 8.5–9.5 nm. The final

data set was restricted to 55 spectral bands, as bands above 900 nm were removed due to very low reflectance.

Two separate data sets were acquired, i.e. one during cloud-free conditions and the other during homogeneous cloud cover. Spectral acquisitions involved internal dark current measurements before each scan to account for systematic scan artefacts. During the scans we recorded the incoming radiance data, which enabled an absolute radiometric calibration to reflectance. The calibration was performed in the ENVI plugin CaliGeoPro (Specim Limited, Oulu, Finland). We averaged the signal from a section of the water surface area free of sun glint or shading. From each curve, a baseline was subtracted measured in clear water in the shaded inside of the tank.

Data acquisition of the boat-based reservoir spectrometry

We transferred and expanded the approach to estimate concentrations during two campaigns (spring and autumn) in the Passauna drinking water reservoir in southern Brazil. We used a 'RoX' instrument (JB Hyperspectral Devices, Düsseldorf, DE) to measure the reflectance of the reservoir. The device is based on a FLAME-S-VIS spectrometer (Ocean Optics, Dunedin FL, USA) and is an advanced development of a spectroscopy setup described in Burkart *et al.* (2014) to perform unsupervised reflectance measurements. The two ends of a bifurcated glass fibre leave the spectrometer point at the nadir and zenith, respectively. The downward-looking fibre measures upwelling radiance within an opening angle of about 20°. Shutters alternately close one and both fibres to measure up- and downwelling radiance as well as dark current in each measuring cycle. After subtracting the dark current, reflectance is calculated as the quotient between downwelling and upwelling radiance. We mounted the spectrometer to a boom stand on a small motor boat (Figure 1). From about 1.2 m above the water surface, the device pointed at the water surface outside the boat shadow and measured reflectance curves in short time intervals (about 10 seconds), while we drove transects across the impoundment. This way, we recorded water surface reflectance curves from 400 to 900 nm with corresponding location and time information. In the presented case, water surface is defined as the part of the water column from which sunlight is reflected back into the upper hemisphere, or the water column above the attenuation depth. In 24–49 reference samples, nine water quality parameters were measured (see Table 1). Only optically deep water was measured.

Target parameters

All water samples were taken from the first 20 cm of the water column. Samples were stored in dark and cold (4 °C) until analysis in the laboratory. The parameters ranged from directly optical active (e.g. TSS) to indirect (e.g. particle bound TP) or optical inactive (e.g. DO) parameters.

For both the mesocosm experiment and the boat-based campaign, TSS concentrations were measured by filtering known volumes of the samples through pre-weighted 0.6 µm glass-fibre filters by means of a vacuum pump, drying them for several hours at 105 °C and weighing them again to obtain the total mass of suspended solids in the sample volume. We then calculated TSS concentrations

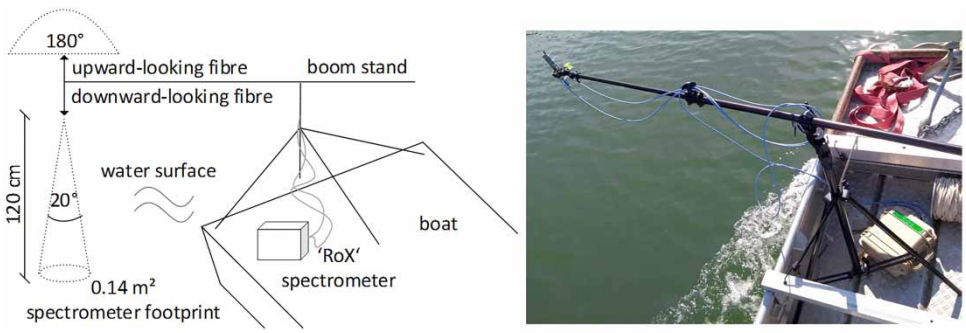

Figure 1 | Left: Diagram of the boat setup used to acquire reflectance measurements at Passauna drinking water reservoir. Right: Photograph of the system during measurement.

Table 1 | Water quality parameters and mean goodness-of-fit-measures of 100-fold iterated PLS regression setups.

Data set	Param.	Unit	*n*	Mean	Min	Max	SD	LV	R^2_{cal}	RP% cal	R^2_{val}	RP% val
$M_{S,2300}$	TSS	mg l^{-1}	12	453	0.00	1,772	793	5	0.99	4.5	0.99	1.7
$M_{Cl,2300}$	TSS	mg l^{-1}	25	458	0.00	2,215	503	5	0.97	4.0	0.98	3.0
$M_{Co,2300}$	TSS	mg l^{-1}	37	456	0.00	2,215	601	5	0.96	5.5	0.97	4.4
$M_{Co,600}$	TSS	mg l^{-1}	25	114	0.00	547	158	5	0.96	5.3	0.99	3.3
$M_{Co,200}$	TSS	mg l^{-1}	20	45.1	0.00	197	59.9	4	0.98	3.7	0.99	2.1
	TSS	mg l^{-1}	31	9.86	0.37	55.7	13.9	2	0.93	6.7	0.95	5.5
	Turbidity	NTU	32	21.0	1.10	131	35.7	3	0.99	2.9	0.99	2.0
	Z_{SD}	m	49	1.67	0.15	3.70	0.98	2	0.71	15	0.77	13
	TP	mg l^{-1}	24	0.06	0.01	0.20	0.08	4	0.97	5.7	0.99	3.8
Res.	chl-*a*	µg l^{-1}	39	5.33	0.01	0.07	0.02	5	0.74	12	0.89	7.6
	PC	µg l^{-1}	38	11.4	1.20	19.5	4.45	5	0.74	12	0.91	7.4
	DO	mg l^{-1}	32	7.87	0.00	47.5	12.8	3	0.73	13	0.82	11
	pH	–	32	7.71	4.81	9.95	1.40	5	0.92	8.1	0.97	5.1
	COD	mg l^{-1}	24	10.7	6.35	8.33	0.65	3	0.14	34	0.45	27

RP%: root mean square error of prediction, given as percentage of the maximum subtracted by the minimum measured value. LV: latent vectors, SD: standard deviation, Res.: reservoir, M: mesocosm with subscripts S (sunny), Cl (cloudy) and Co (combined), numbers indicating TSS range.

by dividing the masses by the respective volumes. Phycocyanin (cyanobacteria proxy), chlorophyll-*a* (green algae) and turbidity were measured *in situ* using TriOS nanoFlu fluorescence sensors and turbidimeter, respectively. DO and the pH were also directly measured in the field using a Horiba U52 multi probe. Z_{SD} was determined by slowly lowering a 25 cm black and white plastic disk into the water until it was no longer visible. TP was analysed colorimetrically using the ascorbic acid method and light absorption at 880 nm (Method 4500-P E). COD was determined by the closed reflux titrimetric method (Clesceri 1998).

Spectral analysis

All spectral data were processed in R (R Core Team 2017). Raw spectra were smoothed using a Savitzky–Golay filter (Savitzky & Golay 1964). Only for the reservoir data, boundary reflectance values for each band were defined based on visual inspections to eliminate distorted spectra. From each reflectance value, we subtracted the mean value of the corresponding curve to minimize the effect of overall curve intensity shifts caused by changing light conditions during the measurement. The first derivative of each curve was determined.

The processed curves and their first derivative were jointly used as predictors for substance concentrations in PLS regression models using the orthogonal scores algorithm. We made use of the R package 'pls' (Mevik & Wehrens 2007). PLS decomposes the entire feature space (here hyperspectral bands) into fewer latent variables that explain the essential variation of the response variable (here substance concentrations) via a linear regression (Wold *et al.* 2001). PLS is thus well suited for the high dimensionality and redundancy in hyperspectral data. Pairs of concentration values and corresponding (mean) spectra were split in a training (75%) and test set (25%) to calibrate and validate the empirical models using cross-validation. This process was iterated 100 times to extract mean goodness-of-fit measures. The models with one to five latent vectors were then evaluated by their root mean square error of prediction (RMSEP) and their R^2 for the test and training sets. The setup with the smallest number of latent vectors and the lowest RMSEP was deemed optimal. For the reservoir data set, the selected PLS was used to estimate concentrations from the remaining spectra which were not used to train or test the model.

RESULTS AND DISCUSSION

The developed work flow and the obtained results from the mesocosm experiments allowed for the transfer of the

described measurement approach to a drinking water reservoir. Results are presented in the corresponding order.

Mesocosm experiment

For both sets collected, an increase of TSS concentrations leads to an increase of reflectance most pronounced in the wavelength regions of 450–550 nm and especially 700–900 nm, the latter with a local maximum at around 815 nm. This is in accordance with previous findings and highlights the importance of the near infrared to detect suspended matter concentrations (Lodhi *et al.* 1998; Knaeps *et al.* 2010; Wu *et al.* 2014). The illumination conditions were found to have a strong impact on the shape of the reflectance curves. Reflectance from diffusive sunlight shows an about three-times steeper increase between 400 and 500 nm. For direct sunlight, the spectra appear flatter. The PLS predictions are best when test and training data sets are acquired under similar illumination conditions (Table 1). However, a regression model built from data from both sets, sunny and overcast (Figure 2), is still well within the performance range of linear or second-order regressions used in similar setups (Lodhi *et al.* 1998). This finding is particularly important for the transfer of the approach to permanent or campaign-based measurements, where changes in illumination conditions happen frequently. From the experiences, frequent measurements of the downwelling irradiance are recommended, ideally one for each measurement of the upwelling radiance. By subsetting the data set, PLS calibrations using smaller TSS concentration ranges (0–200 mg l^{-1} and 0–600 mg l^{-1}) were made (Table 1). The predictive power of these models is in the same range as the model using the entire data set. This suggests that if calibrated accordingly, a wide range of TSS concentrations can be precisely estimated from close-range reflectance measurements.

Boat-based reservoir spectrometry

During subsequent spectra processing, PLS models were built from reflectance spectra and corresponding reference data for several parameters (Table 1). For TSS, the predictive power of the in-field data is only slightly lower compared with the controlled mesocosm experiments. It is also within the range of accuracy reached with designated turbidimeters (Rügner *et al.* 2014). Considering the often less-than-ideal measurement conditions caused by waves, movements of the boat or rapidly changing illumination conditions, the results are encouraging. Even at a boat speed of up to 20 km h^{-1}, usable reflectance curves and hence concentrations could be retrieved. For submerged optical sensors such as turbidimeters, an elaborate mounting and a much slower cruising speed (from our experience less than 5 km h^{-1}) are needed to obtain accurate data. Moving measurements with sensors in the water are likely to be biased by, for example, air bubbles in front of the measurement window. In airborne systems, total sunlight reflection (i.e. glint, on waves) can distort measurements over extensive water surface areas. We measured with a ~0.14 m^2 footprint much closer to the water surface and filtered and normalized the spectra, which minimized the effect of varying amounts of glint within the footprint.

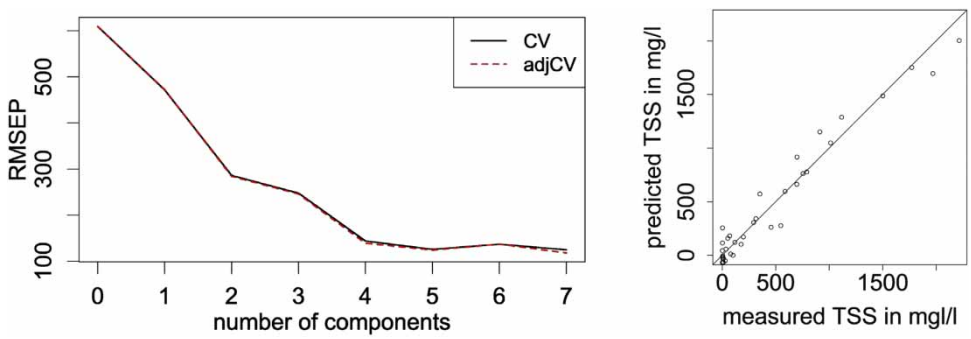

Figure 2 | Results from the PLS regression using combined mesocosm data from sunny and overcast conditions. Left: The RMSEP against the number of components (latent vectors) for cross-validated (CV) and bias-corrected (adjCV) PLS regressions for TSS (mg l^{-1}). Right: Measured against PLS-modelled TSS concentrations using five components ($R^2 = 0.96$).

Although we did not notice pronounced differences in concentration estimated due to changing illumination conditions, measuring during overcast conditions is recommended. Large waves could cause boat movements making measuring at nadir difficult without a gimbal. Also, whitecap conditions should be avoided.

Turbidity, Z_{SD} and TP, the latter being mostly particle-bound, are directly related to TSS concentrations. Due to this covariance, they can be determined with a similar precision as TSS itself. From these parameters, Z_{SD} shows the greatest uncertainty mainly because of the subjective way the reference data is collected. More surprisingly, the data show that the optically inactive parameters DO and pH can also be derived from reflectance with a reasonable precision. It is important to stress at this point, that such specific relations may only be valid for this individual surface water body. At Passauna reservoir, the inflowing and often highly turbid water can have low oxygen contents as well as low pH values. This is likely to be due to oxygen-consuming processes associated with suspended, acidic erosion material. In this case, suspended matter has great proxy capabilities, which may not be the same in other catchments. Spatial and temporal transferability are often pointed out as limitations of empirical procedures like PLS regression (Ritchie *et al.* 2003). In the presented case, the temporal transferability of the approach could be successfully demonstrated. Measurements from spring and autumn were combined in the training and test data sets for the models, which reached a similar precision compared with the models based on just one campaign.

In contrast to the general expectation, the presented approach only shows a fair precision for predicting the optically active substances chl-*a* and phycocyanin, which may have several reasons. At least for chl-*a*, there are only a few higher values and many low concentrations in the data set, which is a less-than-ideal situation for training a model. Furthermore, the reference measurements themselves are based on a (possibly biased) optical procedure, which uses a global calibration of the manufacturer. Lastly, both *in situ* reference sensors for chl-*a* and phycocyanin do not seem optimal for the highly turbid waters of the inflow area, where the sensor readings were less stable than in waters with low TSS concentrations. The influence of turbidity and species composition on optical phycocyanin measurements is described in more detail by Brient *et al.* (2008).

For similar reasons, estimating COD from reflectance in the reservoir does not show good results. Any changes of water surface reflectance due to COD are presumably covered by the dominant changes induced by suspended sediment. Other studies have considered COD a parameter difficult to assess by remote sensing techniques (Gholizadeh *et al.* 2016). For this parameter, absorption-based submerged UV–visible spectrometers are better suited (Torres & Bertrand-Krajewski 2008).

Figure 3 shows the surface TSS concentration estimates based on hundreds of spectral point measurements from a moving boat. Here, the concentration gradient from the reservoir inflow area towards deeper parts of the impoundment is traced. At the narrow point between the shallow inflow (mean depth of about 2 m) area to the north and the deeper main reservoir to the south, the concentration changes rapidly. The presented results show which parts of the reservoir surface are impacted by the TSS input caused by a heavy rain event, or to what extend the inflow area is inhibiting substance flux to the main reservoir. This is valuable information for the reservoir operator, which would have been difficult to obtain with traditional methods.

There need to be considerations for which part of the water column the modelled concentrations are valid. One way to approach this issue is to use the attenuation depth as the lower boundary of the water column layer which contributes to the spectral measurement. It is defined as the depth from which 90% of the water-leaving radiance emerges and can be calculated from attenuation

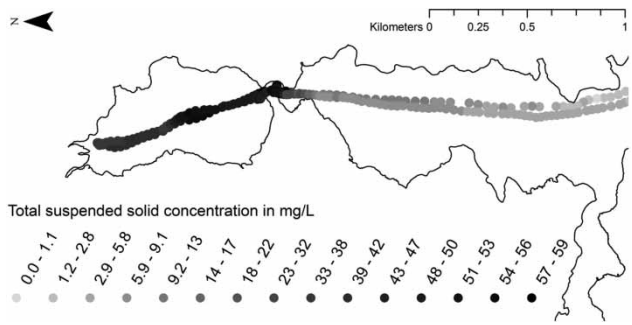

Figure 3 | TSS concentration gradient in the inflow area and northern part of Passauna reservoir (Brazil) based on spectral measurements and PLS modelling.

measurements. If such measurements are not available, Z_{SD} can be used as a proxy to calculate the attenuation coefficient and subsequently attenuation depth. Using the nonlinear equation for neotropical systems introduced by Padial & Thomaz (2008), the attenuation depth in Passauna reservoir ranges from 0.12 m (Z_{SD}: 0.15 m) in the highly turbid buffer to 1.37 m (Z_{SD}: 3.7 m) near the dam. Even though the presented method is either limited to the uppermost layer of stagnant water bodies or relies on the full mixing of water bodies, like in rivers, the characterization of the epilimnion (e.g. trophic state) serves as crucial information for reservoir management.

To further improve the understanding of implications between the uppermost water layer and deeper volumes, we are currently examining the combination of proximal spectroscopy and acoustic backscatter measurements from the same boat to cover the entire water column. The concentration estimates from the spectrometer can be used as calibration for the acoustic data, which is only able to record relative intensities. The spectra can also be used as reference for remote sensing techniques such as multi- and hyperspectral drone and satellite imagery.

CONCLUSIONS AND OUTLOOK

We tested close-range water reflectance measurements to retrieve water quality parameters under different illumination conditions in a mesocosm experiment and from a boat in a reservoir. The method is suitable and time-saving for parameters directly influencing the reflection properties of the water body, or for parameters closely related to those. Possible applications are campaign-based spectral measurements from mobile platforms like boats and drones as well as stationary deployment at weirs, bridges or on buoys for lake and river monitoring. Empirical procedures like PLS are highly sensitive to the training data used and their validity must be monitored, especially when applied to other regions or seasons. Alternatively, physical-based modelling can be considered to retrieve concentrations from spectral measurements. As next steps, the integration of the method with remote sensing imagery and with acoustic data will be investigated, as a high temporal and spatial resolution for monitoring the water surface and water column is pursued. In this context, we believe that above-surface water spectrometry is a valuable contribution to monitoring and mapping water quality in rivers, reservoirs and lakes.

ACKNOWLEDGEMENTS

Research was supported by the Graduate School for Climate and Environment (grace.kit.edu). Stefan Hinz of the KIT-IPF is thanked. We thank Tobias Bleninger, Cristovão Fernandes, Heloise Knapik and the staff of UFPR-DHS (dhs.ufpr.br). Thanks go out to Mauricio Scheer and the staff of SANEPAR (site.sanepar.com.br). Andreas Burkart of JB Hyperspectral (jb-hyperspectral.com) is thanked.

REFERENCES

Apitz, S. & White, S. 2003 A conceptual framework for river-basin-scale sediment management. *Journal of Soils & Sediments* **3** (3), 132–138.

Brient, L., Lengronne, M., Bertrand, E., Rolland, D., Sipel, A., Steinmann, D., Baudin, I., Legeas, M., Le Rouzic, B. & Bormans, M. 2008 A phycocyanin probe as a tool for monitoring cyanobacteria in freshwater bodies. *Journal of Environmental Monitoring* **10** (2), 248–255.

Burkart, A., Cogliati, S., Schickling, A. & Rascher, U. 2014 A novel UAV-based ultra-light weight spectrometer for field spectroscopy. *IEEE Sensors J.* **14** (1), 62–67.

Clesceri, L. S. 1998 *Standard Methods for the Examination of Water and Wastewater*, 20th edn. American Public Health Assoc., Washington, DC, USA.

Gholizadeh, M. H., Melesse, A. M. & Reddi, L. 2016 A comprehensive review on water quality parameters estimation using remote sensing techniques. *Sensors* **16** (8), 1298.

Horowitz, A. J. 2013 A review of selected inorganic surface water quality-monitoring practices: are we really measuring what we think, and if so, are we doing it right? *Environmental Science & Technology* **47** (6), 2471–2486.

Knaeps, E., Sterckx, S. & Raymaekers, D. 2010 A seasonally robust empirical algorithm to retrieve suspended sediment concentrations in the Scheldt River. *Remote Sensing* **2** (9), 2040–2059.

Lodhi, M. A., Rundquist, D. C., Han, L. & Kuzila, M. S. 1998 Estimation of suspended sediment concentration in water using integrated surface reflectance. *GeoCarto International* **13** (2), 11–15.

Martínez-Carreras, N., Schwab, M. P., Klaus, J. & Hissler, C. 2016 *In situ* and high frequency monitoring of suspended sediment properties using a spectrophotometric sensor. *Hydrological Processes* **30** (19), 3533–3540.

Mevik, B.-H. & Wehrens, R. 2007 The pls package: principal component and partial least squares regression in R. *Journal of Statistical Software* **18** (2), 1–23.

Padial, A. A. & Thomaz, S. M. 2008 Prediction of the light attenuation coefficient through the Secchi disk depth: empirical modeling in two large Neotropical ecosystems. *Limnology* **9** (2), 143–151.

R Core Team 2017 *R: A Language and Environment for Statistical Computing*. R Foundation for Statistical Computing, Vienna, Austria.

Ritchie, J. C., Schiebe, F. R. & McHenry, J. R. 1976 Remote sensing of suspended sediments in surface water. *Photogrammetric Engineering and Remote Sensing* **42** (12), 1539–1545.

Ritchie, J. C., Zimba, P. V. & Everitt, J. H. 2003 Remote sensing techniques to assess water quality. *Photogrammetric Engineering and Remote Sensing* **69** (6), 695–704.

Rügner, H., Schwientek, M., Egner, M. & Grathwohl, P. 2014 Monitoring of event-based mobilization of hydrophobic pollutants in rivers: calibration of turbidity as a proxy for particle facilitated transport in field and laboratory. *Science of the Total Environment* **490**, 191–198.

Savitzky, A. & Golay, M. J. E. 1964 Smoothing and differentiation of data by simplified least squares procedures. *Analytical Chemistry* **36** (8), 1627–1639.

Schalles, J. F., Rundquist, D. C. & Schiebe, F. R. 2001 The influence of suspended clays on phytoplankton reflectance signatures and the remote estimation of chlorophyll. *Verhandlungen des Internationalen Verein. Limnologie (SIL Proceedings (1922–2010))* **27** (6), 3619–3625.

Silván-Cárdenas, J. L. & Wang, L. 2010 Retrieval of subpixel *Tamarix* canopy cover from Landsat data along the Forgotten River using linear and nonlinear spectral mixture models. *Remote Sensing of Environment* **114** (8), 1777–1790.

Torres, A. & Bertrand-Krajewski, J.-L. 2008 Partial Least Squares local calibration of a UV–visible spectrometer used for *in situ* measurements of COD and TSS concentrations in urban drainage systems. *Water Science and Technology* **57** (4), 581–588.

Wold, S., Sjöström, M. & Eriksson, L. 2001 PLS-regression: a basic tool of chemometrics. *Chemometrics and Intelligent Laboratory Systems* **58** (2), 109–130.

Wu, J.-L., Ho, C.-R., Huang, C.-C., Srivastav, A. L., Tzeng, J.-H. & Lin, Y.-T. 2014 Hyperspectral sensing for turbid water quality monitoring in freshwater rivers: empirical relationship between reflectance and turbidity and total solids. *Sensors* **14** (12), 22670–22688.

First received 11 June 2018; accepted in revised form 15 October 2018. Available online 29 October 2018